

4.3 An Investigation of Nocturnal low-level-jet generated gravity waves and turbulence over Oklahoma City during JU2003

Yansen Wang*, Cheryl Klipp, Chatt Williamson, Giap Huynh
Dennis Garvey, Sam Chang

US Army Research Laboratory, Adelphi, MD 20783

1. INTRODUCTION

The Joint Urban 2003 (JU2003) project, a cooperative undertaking to study turbulent transport and diffusion in urban atmospheric boundary layers, was conducted in Oklahoma City (OKC) in June and July of 2003 (Allwine, 2003). Boundary layer wind data observed by Doppler lidar over Oklahoma City during the JU2003 indicate that a strong nocturnal low-level-jet (LLJ) dominated the boundary layer flows during the early morning hours of most of the intensive observation days. Gravity waves appeared in this type of flow in the late morning due to the strong shear of the LLJ and the weak temperature stratification below the jet. In this paper, we intend to study the LLJ-generated gravity waves by analyzing the sonic anemometer, Doppler lidar, and radiosonde observational data. The mechanism of the gravity wave generation by the LLJ is investigated using a linear stability analysis. The wavelength and phase speed of the wave are computed using the spectral and wavelet methods. The wind signals are separated into waves and turbulence using a wavelet decomposition method. The momentum fluxes due to the wave motions and turbulent fluctuations are computed.

2. INSTRUMENTATION

Two Doppler lidars, operated by the Army Research Laboratory (ARL) and Arizona State University (ASU) respectively, and a large number of sonic anemometers were deployed to monitor the wind field during the experiment. The Lawrence Livermore National Laboratory (LLNL) set up an 83m high tower with 8 sonic anemometers, which is located at the northern edge of the central business district (Lundquist et al., 2004). The Doppler lidars deployed in the project are WindTracer® Systems, products of the Coherent Technologies, Inc. in Lafayette, Colorado. The systems were designed

specifically for atmospheric boundary layer observations and research. The laser system is operated at a wavelength of 2025nm with 2.5 μ J laser pulse energy. The pulse repetition is 48Hz and the gate range varied from 66 to 71m depending upon the data set. The system measures range-gate resolved backscatter intensity and the Doppler radial velocity. The location of the ARL lidar is shown in Fig. 1, where the lidar was set up on top of a two story parking garage (Global Position System (GPS) coordinate: N35° 28.385', W 97° 30.266', 20m above ground). The ASU lidar was located southeast of OKC (GPS coordinate: N35°26.330', W97°29.553'), about 3.8km from the downtown Central Business District (CBD) out of the domain shown in Fig.1. Both systems functioned well during JU2003, and a large

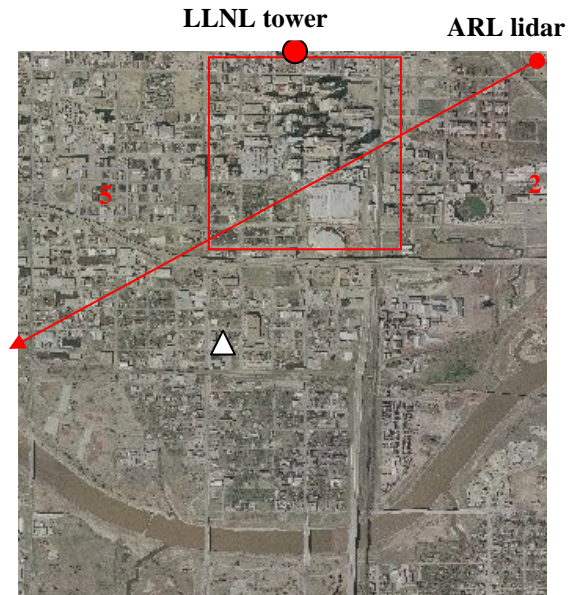


Fig.1 Aerial photograph showing the ARL lidar site and LLNL 83m tower site. The red square is the central business district (CBD) of Oklahoma City. The red arrow line indicates the laser beam. The numbers 2 and 5 show the locations of the ARL 10m towers. ARL towers 1, 3, and 4 are out of range of the aerial photograph. Δ is the PNNL radiosonde release site.

*Corresponding author: Yansen Wang, AMSRD-ARL-CI-EM, U.S. Army Research Lab., Adelphi, MD 20783. email: ywang@arl.army.mil

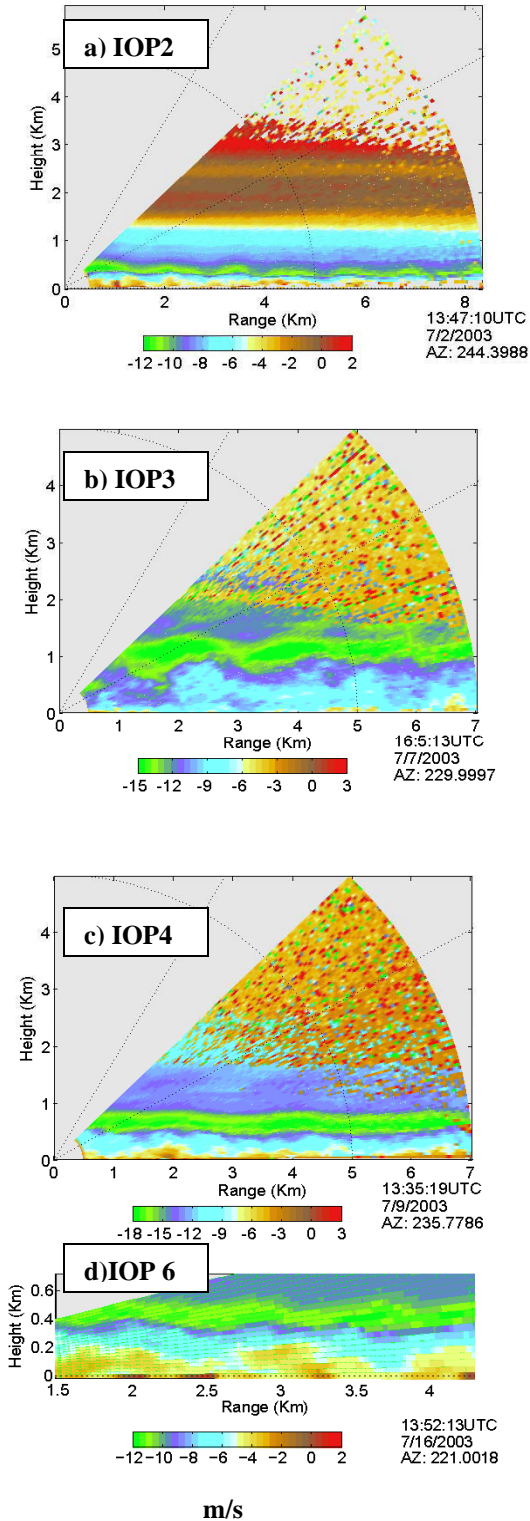


Fig. 2 ARL lidar RHI scan images shows the evident of LLJ and gravity waves during IOP2, 3, 4 and 6. The negative wind denotes the wind is blowing into lidar.

amount of data was collected. In addition, we use the radiosonde observation data taken by the Pacific Northwest National Laboratory (PNNL, De Wekker et al., 2004) for the temperature profile.

3. DATA AND ANALYSIS

LLJs were very common in the clear, undisturbed nights and early mornings during JU2003. Except for IOP1 (Intensive Observation Period) which had convective disturbance, LLJs appeared in other 9 IOPs (De Wekker et al., 2004). From a lidar data analysis, it appears that the LLJ gradually dissipated during the stable to convective boundary layer transition Wang et al., 2005). Before the LLJs are destroyed by the underlying convective boundary layer growth, there is a period during which the atmospheric stability conditions promote shear-generated gravity waves. Evidently, the gravity waves were fairly common during the transition period associated with the growing of the convective boundary layer. Fig.2 shows the RHI (range-height-indicator) scan images of IOP 2, 3, 4, and 6, in which the wave motions appeared. The transition time for IOP5 happened earlier (around 1130 UTC), we didn't have lidar

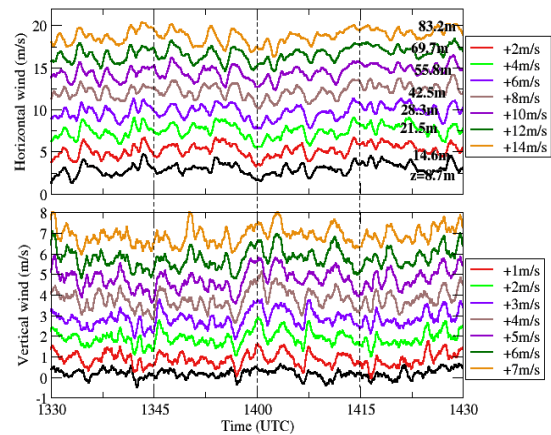


Fig.3 Horizontal winds(top panel) and vertical wind (bottom panel) time series from LLNL tower sonic anemometers during IOP 2. The signals are low-pass filtered to 0.01Hz. The heights of anemometers are labeled on the color coded curves, applying for both panels. The signals are also transformed by adding a number at higher levels to be readable.

data during that time. Although the wavelengths and heights of the LLJ in those waves are

different, they show some similarity in distinct wave motion.

For brevity, the following analysis will only show results from gravity wave episode during the IOP2 (Fig 2a). Fig.3 shows the LLNL tower sonic anemometer observed horizontal and vertical winds during the IOP2 after a low-pass filter (frequency less than 0.01 Hz). Obviously, the LLJ at an upper level generated gravity waves are shown in-situ sonic anemometer winds. The wave motion appeared in both the horizontal and vertical wind signals. U and W were in apparent quadrature with U ahead of W, which is a typical signature of wave motion. Further inspection of the wave signals indicated that the wave was originated at higher levels, with the lower level signals lagging behind. This is consistent with the lidar RHI scan image (Fig. 2a), which shows that wave and low level jet core is at height of 250-350m. The wave signals at different levels also show a damping effect with smaller amplitudes in lower levels. Gravity waves have been observed in nocturnal boundary layers (Blumen et al., 2001; Newsom and Banta, 2003; Sun et al., 2003; Fritts et al., 2003). They have also been found in the transition period (from stable to unstable) boundary layer (Nappo et al., 2002).

3.1 Low-level jet and wave generation

The height of the wave generation appeared to be related to the LLJ height. Fig. 4 is an average vertical profile of horizontal wind retrieved from lidar RHI scans and the potential temperature data from the PNNL radiosonde. The data shows that the strongest shear of the jet is located just below the jet nose or maxima. The potential temperature profile indicated that a near neutral stratification existed below the jet nose at the time. There was a strong stable stratification layer right at the jet nose height. The turbulence intensity (Fig. 4b) is much greater below the jet due to the near neutral stratification. Using the averaged horizontal wind profile and temperature profiles (Fig. 4a,c), the gradient Richardson (Ri) number profile is computed (Fig. 4d). The Richardson number shows a slight unstable condition below 0.15km and almost neutral conditions from 0.15km to LLJ nose (0.35km). Just above the LLJ nose, there is a stable layer where the Ri is much greater than 0.25, which is the critical value (Miles and Howard, 1964) for the development of instability. At this critical point, the instability starts and therefore the gravity wave appears. Indeed, the lidar images (Fig. 2) indicated that the wave motion appeared in the lower levels, but it was damped out above the LLJ.

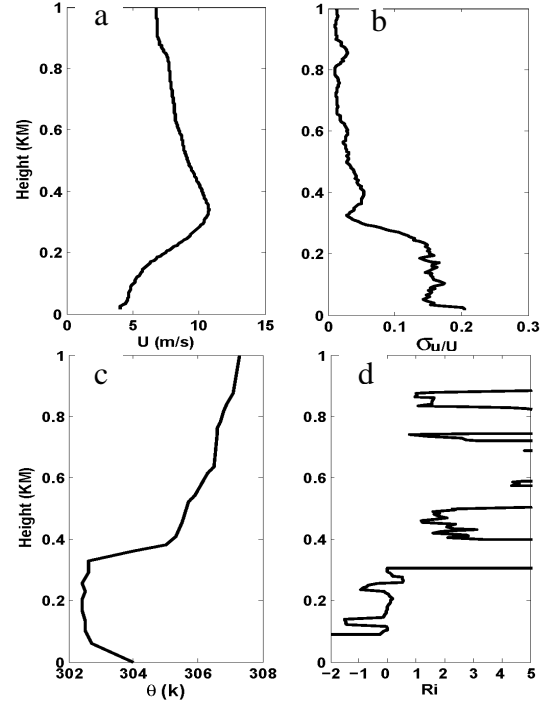


Fig. 4 Lidar averaged horizontal wind speed (a), the spatial variation of horizontal wind(b), the PNNL radiosonde observed potential temperature (c), and computed Ri number around 1419 UTC, IOP2.

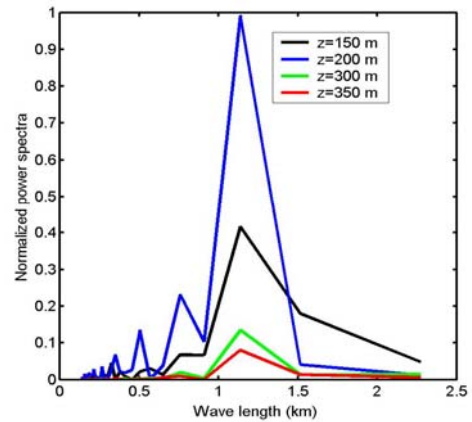


Fig. 5 Power spectra results from lidar retrieved horizontal wind at different heights.

The wave length is very much related to the depth of the shear layer, i.e. the height of the LLJ. The typical wave length from $2\pi h$ to $7.5h$ where h is the depth of the shear layer from a linear analysis theory (Miles and Howard, 1964).

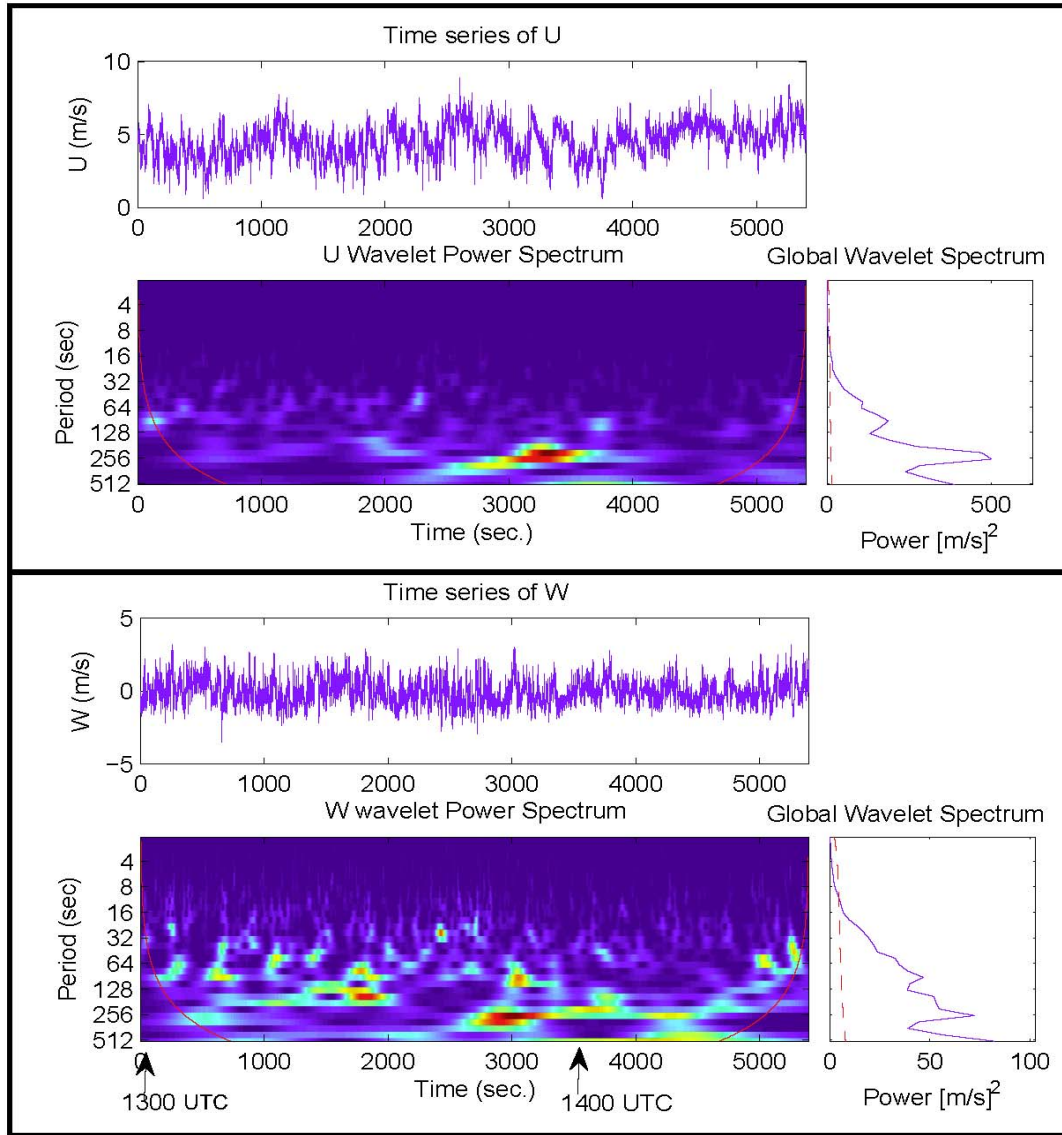


Fig. 6 Wavelet analysis of the horizontal wind (top panel) and vertical wind (bottom panel). The Morlet wavelet is used. Outside of solid red line in wavelet power spectrum diagrams indicates that the edge effects become important. The contour levels range from 1 (dark blue) to 5000 (red). Dashed red line is the 95% confidence level for the global wavelet spectrum.

The wave length from the lidar RHI scan indicated that observational results basically agree with the linear theory. Fig. 5 is a plot of the spectral analysis of the lidar retrieved horizontal wind speed. It indicated that the wave length was around 1.2 km.

The wave motions were also detected from the in-situ point sensor observations. The time series signals from the sonic anemometers were analyzed to characterize the wave motion and its frequency. The wavelet technique is considered one of the most powerful methods to detect signals with different scales (Torrence and Compo, 1998). The wind time series containing different scales of motion can be analyzed using this method. Fig. 6 is wavelet analysis results of LLNL tower top (83m) anemometer signals. The Morlet base wavelet is used for the analysis. The localized wavelet spectrum indicated a wave signature with a period of about 256 second in the U wind signal at 1330-1400 UTC. The W wind showed a similar wavelet spectrum signature, but not as distinct as the U wind. The global wavelet spectrum, which is equivalent to the power spectrum from a Fourier transform, showed a peak around period of 256 seconds. Given the wave propagation is in the order of average wind speed of 5m/s, the 1.28km wave length agrees with the lidar RHI scanning.

3.2 Wave and turbulence momentum fluxes

The gravity wave not only feeds energy to turbulence of small scales through the wave breaking and instabilities, it also directly contributes to the transport of momentum. Figs. 1 and 2 show that coherent wave motions are visible from their originating height to the ground surface. One of difficulty in the study of turbulence and wave interactions is how to separate the turbulence from the waves, especially gravity waves with different frequencies. Finnigan et al. (1984) has used a spectral analysis method to pinpoint the wave frequency and decomposed the wind signal into mean, wave and turbulence components. In the following analysis, we use a wavelet decomposition technique. A Daubechies wavelet base function (Daubechies, 1992) is used for the decomposition. The advantage of the wavelet decomposition is that it can deal with a non-stationary time series.

Fig. 7 shows an example of wavelet decomposition of u signal at z=8.7m into three parts, the mean, the wave (~) and turbulent fluctuation ('). Other components of velocity are also decomposed in the same way. This separation of wave and turbulence allows us to compute individual

momentum fluxes contributed by waves and turbulence (Fig. 8). The wave momentum flux is 3 times greater than the turbulent momentum flux at higher levels and approaches it in magnitude near the ground surface. The negative sign indicates that wave momentum is transported to the ground and is absorbed by the ground surface. Part of the wave momentum may be transferred to the turbulent flux via wave breaking. A detailed energy budget analysis of wave and turbulence is beyond the scope of this paper. It will be investigated in further studies.

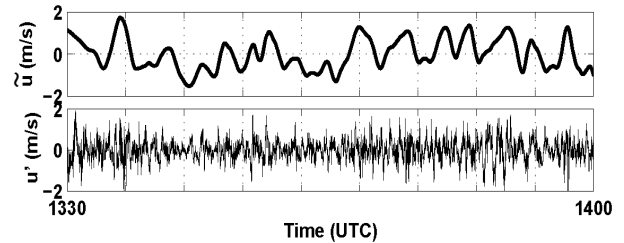


Fig. 7 An example of wavelet decomposition of u wind components. It is decomposed into mean, wave (~), and turbulent fluctuation (') parts.

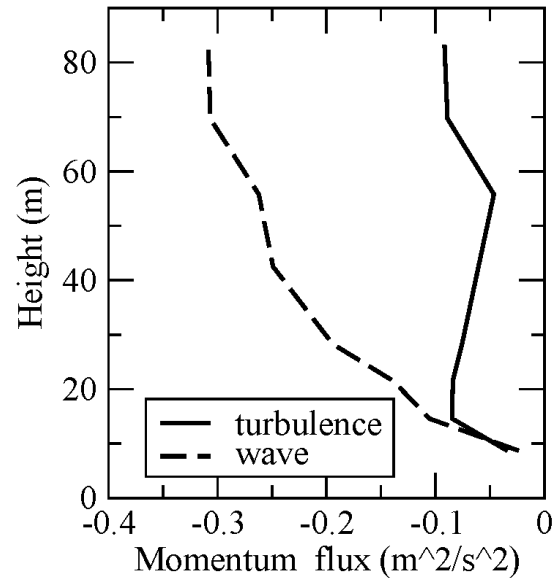


Fig. 8. Wave momentum flux and turbulent momentum flux using the decomposed signals.

4. SUMMARY

Doppler lidar RHI scans and in-situ wind sensors have indicated that linear waves exist during the transition periods from stable to convective boundary layer in the morning hours of JU2003. In the non-disturbed condition, the

LLJ is a dominant flow feature over OKC during the night to morning hours. The LLJ has a large shear from jet maximum to ground. When the temperature stratification is favorable during the boundary layer transition period, the gradient Richardson number is reduced below the critical value of 0.25 and gravity waves are generated. The analysis of wavelength and phase speed using the wavelet method indicates that the waves are approximately linear and agree with the standard linear theory. The wind signals from sonic anemometers are decomposed into the wave and turbulence parts using a wavelet technique. The corresponding wave momentum flux and turbulence momentum flux are computed.

Acknowledgements. We thank the JU2003 organizers and participants for their support. We also thank colleagues at LLNL and PNNL for making the data available in this study. Special thanks are extended to our colleagues in ARL for their dedicated efforts during the JU2003.

References

- Allwine, K. J., M. J. Leach, L. W. Stockham, J. S. Shinn, R. P. Hosker, J. F. Bowers, J. C. Pace, 2004: Overview of joint urban 2003-An atmospheric dispersion study in Oklahoma City. *AMS Symposium on planning, nowcasting and forecasting in urban zone(on CD)*. Seattle, WA, Amer. Meteor. Soc.
- Blumen, W., R. Banta, S. P. Burns, D. Fritts, R. Newsom., G. Poulos, and J. Sun, 2001: Turbulence statistics of a Kelvin-Helmholtz billow event observed in the night time boundary layer during the Cooperative Atmosphere-Surface exchange study field program. *Dyn. Atmos. Oceans*, 34:189-204.
- De Wekker, S. F. J., L. K. Berg, J. Allwine, J. C. Doran, W. J. Shaw, 2004: Boundary-layer structure upwind and downwind of Oklahoma city during the Joint Urban 2003 field study. *AMS 5th conf. on urban environment*. 23-27 August 200, Vancouver, B.C., Canada.
- Daubechies, I., 1992: *Ten lectures on wavelets*. Soc. For Industrial and Applied Math. 357pp.
- Finnigan, J. J., F. Einaudi, and D. Fua, 1984: The interaction between an internal gravity wave and turbulence in the stably-stratified nocturnal boundary layer. *J. Atmos. Sci.*, 41, 2409-2436.
- Fritts, D. C., C. Nappo, D. M. Riggan, B. B. Balsley, W. E. Eichinger, and R. Newsom, 2003: Analysis of ducted motions in the stable nocturnal boundary layer during CASES-99. *J. Atmos. Sci.*, 60, 2450-2472.
- Lundquist, J. K., J. H. Shinn, and F. Gouveia, 2004: Observations of turbulent kinetic energy dissipation rate in the urban environment. *AMS Symposium on planning, nowcasting and forecasting in urban zone(on CD)*. Seattle, WA, Amer. Meteor. Soc.
- Miles, J. W., L. N. Howard, 1964: Note on heterogeneous shear flow. *J. Fluid Mech.*, 20: 331-336.
- Nappo, J. C., R. Doboay, and E. Dumas, 2002: Wave and turbulence observed over two consecutive VTMX nights, *10th Conference on Mountain Meteorology and MAP Meeting*. Seattle, WA, Amer. Meteor. Soc.
- Newsom, R. K. and R. M. Banta, 2003: Shear-flow instability in the stable nocturnal boundary layer as observed by Doppler lidar during CASES-99. *J. Atmos. Sci.*, 60, 16-33.
- Sun, J. and coauthors, 2003: Atmospheric disturbances that generate intermittent turbulence in nocturnal boundary layer. *Boundary-layer meteorol.*, 110:255-279.
- Torrence, C and P. Compo, 1998: A practical guide to wavelet analysis. *Bull. Amer. Meteorol. Soc.* 79: 61-78.
- Wang, Y., C. Klipp, C. Williamson, D. Ligon, Y. Yee, D. Garvey, S. Chang, R. Newsom, R. Calhoun, 2005. Nocturnal Low-level-jet Dominated Atmospheric Boundary Layer Observed by Doppler Lidars over Oklahoma City during JU2003. Submitted to *J. Appl. Meteorol.*